phys. stat. sol. (b) **63**, 699 (1974)

Subject classification: 18.4; 22.8

Nuclear Research Center-Negev, Beer-Sheva, Israel

Magnetic Structure of $CsCoCl_3$ at 4.2 °K

By

M. MELAMUD, H. PINTO, J. MAKOVSKY, and H. SHAKED

The compound $CsCoCl_3$ is paramagnetic at room temperature and belongs to the space group D_{6h}^4–$P6_3/mmc$ with two formula units per unit cell ($CsNiCl_3$ type structure). The neutron diffraction of $CsCoCl_3$ powder and single crystal samples were studied as a function of sample temperature. A transition to antiferromagnetism was found at $T_N = 21.5$ °K. The magnetic structure determined from the diffraction pattern at 4.2 °K is collinear and consists of ferrimagnetic ab planes stacked antiferromagnetically along the c-axis with spins parallel to the c-axis. The magnetic moment consistent with the diffraction at 4.2 °K is (3.0 ± 0.3) and (2.3 ± 0.3) Bohr magnetons per Co^{2+} ion according to the powder and single crystal data, respectively. The magnetic unit cell is the hexagonal H-cell ($a = \sqrt{3}a_0$, $c = c_0$) with six formula units per unit cell. This structure belongs to the magnetic space group $P6_3'/m'cm'$ (III_{193}^{259}–$P6_3'/m'cm'$). The powder and single crystal data show that the magnetic structure near T_N is different from the magnetic structure at 4.2 °K.

Le composé $CsCoCl_3$ est paramagnétique à la température ambiante, et appartient au groupe spatial D_{6h}^4–$P6_3/mmc$ comportant deux unités de $CsCoCl_3$ par maille élémentaire (structure type $CsNiCl_3$). Le spectre de diffraction des neutrons a été étudié en fonction de la température pour le composé $CsCoCl_3$ sous forme de poudre ainsi que sous forme de monocristaux. Un point de transition antiferromagnétique a été observé à la température $T_N = 21{,}5$ °K. La structure magnétique déterminée à partir du spectre de diffraction à 4,2 °K, est colinéaire et comporte des plans ab ferrimagnétiques empilés antiferromagnétiquement dans la direction c, les spins étant parallèles à cette direction. La maille élémentaire magnétique est la cellule – H héxagonale ($a = \sqrt{3}a_0$, $c = c_0$) comportant six unités de $CsCoCl_3$. Cette structure appartient au groupe spatial $P6_3'/m'cm'$ (III_{193}^{259}–$P6_3'/m'cm'$). Les résultats obtenus à partir d'échantillons monocristaux et sous forme de poudre indiquent que la structure magnétique aux alentours de T_N es différente de celle à 4,2 °K.

1. Introduction

The compound $CsCoCl_3$ is perovskite related and is isomorphous with $CsNiCl_3$ [1 to 4]. It has a hexagonal two layer (2L) structure which at room temperature (RT) belongs to the space group $D_{6h}^4 - P6_3/mmc$, having two formula units per unit cell [2 to 4]. It is built up of linear chains of face sharing octahedra of Cl^- along the c-axis, with the Co^{2+} ions positioned at the centre of these octahedra. The Cs^+ with the Cl^- ions form $(CsCl_3)^{2-}$ sheets perpendicular to the c-axis. Table 1 a gives the ions positions in this structure.

Several compounds isomorphous with $CsNiCl_3$ were previously investigated and their magnetic structures were determined [5 to 13]. These compounds are listed in Table 2 and classified according to the seven types of magnetic structures which were found. The types of magnetic structures are defined in Table 3.

The compound $CsCoCl_3$ was investigated by NMR [14], magnetic susceptibility [3, 15], and ESR [15]. Achiwa [15] concluded from the crystallographic structure and from the broad maximum in his susceptibility measurement, that $CsCoCl_3$ has linear antiferromagnetic chains along the c-axis. This conclusion is

also consistent with the results of his measurement of the exchange interaction perpendicular and parallel to the c-axis which gave $J_{\parallel} > J_{\perp}$. Ferromagnetic chains were found among the isomorphous compounds only in $CsNiF_3$ [16] whereas antiferromagnetic chains were found in all the rest. In this work we show that the three-dimensional magnetic structure of $CsCoCl_3$ at 4.2 °K (see Fig. 2) indeed consists of antiferromagnetic linear chains.

2. Experimental

The compound $CsCoCl_3$ was prepared by melting stoichiometric amounts of CsCl and anhydrous $CoCl_2$ in an evacuated quartz ampoule. The CsCl used was a Merck u.p. material, dried in a vacuum desiccator. The anhydrous $CoCl_2$ was prepared from (Merck G.R.) hydrated material by heating it in a HCl stream. The X-ray powder pattern of the resulting blue product showed no lines other than those of the pure material [3, 4]. Chemical analysis of the Co^{2+} ions was carried out by the EDTA complexometric titration and that of the Cl^- ions by argentometric titration. Results of the chemical analysis are: Co^{2+} 19.6 wt% (calculated 19.76 wt%); Cl^- 35.6 wt% (calculated 35.66 wt%).

Neutron ($\lambda = 1.02$ Å) diffraction patterns of a powder sample of $CsCoCl_3$ were taken at room and liquid helium temperatures (RT and LHeT, see Fig. 1). Indexing of the RT pattern is according to the unit cell given by Soling [3]

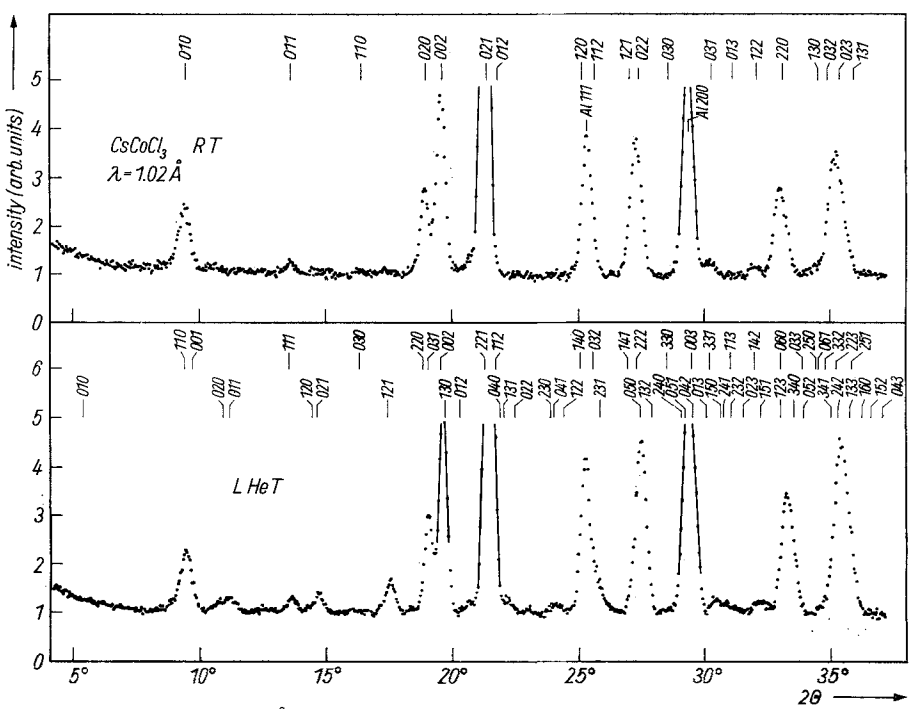

Fig. 1. Neutron ($\lambda = 1.02$ Å) diffraction patterns of $CsCoCl_3$ at room and liquid helium temperatures (RT and LHeT). Indexing of the RT patterns is according to the unit cell given by Soling [3] and only allowed reflections in $P6_3/mmc$ are shown. Indexing of the LHeT pattern is according to the H-cell (Fig. 2). Indices of lattice and of superlattice lines are given in the upper and lower rows respectively

($a_0 = 7.2019$ Å, $c_0 = 6.0315$ Å), which is within error limits of those given by others [2, 4].

Using a least square computer program, a minimalization of the residual R[1]) was carried out to fit the calculated to the observed integrated intensities of 14 lines in the RT pattern. This calculation resulted in the ion positions given in Table 1a, with an overall temperature (Debye-Waller) factor[2]) $B = (2.1 \pm 0.7)$ Å^2, and a residual $R = 8\%$. The value of the position parameter x

Table 1

Structural data for $CsCoCl_3$. a_0 and c_0 are according to [3]. The positional parameters are the results of a least square analysis of the integrated intensities at room temperature

a)	$P6_3/mmc$,	$a_0 = 7.2019$ Å,			$c_0 = 6.0315$ Å								
	2 Co in (a)	0	0	0;	0	0	1/2						
	2 Cs in (d)	±(1/3	2/3	3/4)									
	6 Cl in (h)	±(x	$2x$	1/4;	$2\bar{x}$	$\bar{x}$	1/4;	x	$\bar{x}$	1/4)			
		with $x = 0.155 \pm 0.002$											
b)	$P6_3/mcm$,	$a = \sqrt{3}a_0$,			$c = c_0$								
	2 Co in (b)	0	0	0	0	0	1/2						
	4 Co in (d)	(1/3	2/3	0;	2/3	1/3	0;	1/3	2/3	1/2;	2/3	1/3	1/2
	6 Cs in (g)	±(x	0	1/4;	0	x	1/4;	$\bar{x}$	$\bar{x}$	1/4)			
		with $x = 1/3$											
	6 Cl in (g)	with $x = 0.845 \pm 0.002$											
	12 Cl in (j)	±(x	y	1/4;	$\bar{y}$	$x-y$	1/4;	$y-x$	$\bar{x}$	1/4)			
		±(y	x	1/4;	$x-y$	$\bar{y}$	1/4;	$\bar{x}$	$y-x$	1/4)			
		with $x = 0.488 \pm 0.002$						$y = 0.821 \pm 0.002$					

is equal (within error bounds) to the X-ray value reported by Soling [3]. The values of the nuclear scattering amplitudes used are: $b(Cs) = 0.55$ [17], $b(Co) = 0.25$ [18], and $b(Cl) = 0.96$ [18] (in units of 10^{-12} cm).

Three superlattice lines which did not appear in the RT pattern were observed (Fig. 1) in the LHeT pattern. The smallest unit cell which corresponds to these lines is the hexagonal H-cell [19] with $a = a_0\sqrt{3}$ and $c = c_0$ (Fig. 2). This cell contains six formula units of $CsCoCl_3$. The magnetic structure compatible with the LHeT pattern (as is shown in the next section) consists of collinear ferrimagnetic planes stacked antiferromagnetically along the c-axis (Fig. 2). The space group consistent with the LHeT pattern is D^3_{6h}-$P6_3/mcm$, and the magnetic structure belongs to the magnetic space group $P6'_3/m'cm'$. A comparison of the LHeT to the RT nuclear lines at large 2θ, shows a monotonic increase in intensity with 2θ (Fig. 1). This increase can be accounted for by the decrease of B to zero (at 4.2 °K). Hence, it was assumed that the ionic positions do not change as the sample is cooled from RT to LHeT. The coordinates corresponding to $P6_3/mcm$ of the positions at LHeT are listed accordingly in Table 1b. This assumption was subsequently verified (within error bounds) by minimalization of R in fitting the nuclear and magnetic calculated to the observed integrated

[1]) The residual is defined by

$$R = 100\ \{\Sigma\,[I_{obs} - I_{calc}]/\sigma]^2/\Sigma\,[I_{obs}/\sigma]^2\}^{1/2}\,,$$

where σ is the estimated error in I_{obs}.

[2]) The overall temperature factor B, is defined by $I_{hkl} = I_{calc} \exp(-B/2d^2)$, where d is the interplanar distance of the hkl planes.

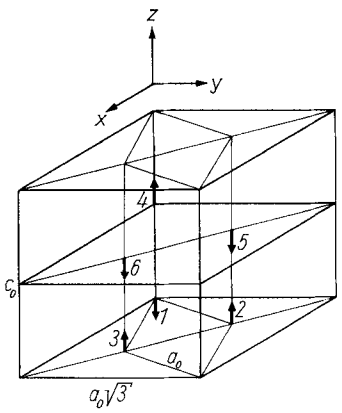

Fig. 2. Magnetic unit cell (H-cell) of $CsCoCl_3$. The of spins the Co^{2+} ions are shown

intensities of 23 lines in the LHeT pattern. This fit resulted in a residual $R = 10\%$. The number of Bohr magnetons for the Co^{2+} ions resulting from this fit is $(3.0 \pm 0.3)\,\mu_B$. The form factor used is $\exp(-8.3[\sin\theta/\lambda]^2)$, which fits the data given by Watson and Freeman [20].

The peak intensities of the magnetic lines measured as a function of temperature (Fig. 3) and the Néel temperature was found to be (21.5 ± 0.5) °K. The intensity versus temperature curves for all (i.e. {011}, {021}, and {121} magnetic reflections exhibit an anomaly at about 8 °K. Intensity-temperature curves of (011), (021), (041), and (051) $(2h + k \neq 3n)$ obtained with a single crystal are similar to the {121} curve (for powder) shown in Fig. 3. The single crystal

Table 2

Compounds isostructural with $CsNiCl_3$, classified according to their magnetic structure

magnetic structure type	compound	T_N (°K)	ref.
I	$BaMnO_3$	<2.4	[5]
	$CsCoCl_3$	21.5	*)
	$RbCoBr_3$	36	[6]
	$CsCoBr_3$**)	≈15	[7]
	$RbNiCl_3$	11	[8]
II	$CsCoBr_3$**)	28	[7]
III	$CsCoBr_3$**)	28	[7]
IV	$CsNiF_3$	2.65	[9]
V	$CsMnBr_3$	8.3	[10]
	$RbFeCl_3$	2.55	[11]
VI	$CsNiCl_3$	4.5	[12]
	$RbNiCl_3$	11	[12]
VII	$RbMnBr_3$	8.8	[13]

*) The present work.

**) Structure I was proposed for this compound at 4.2 °K, whereas, structures II or III were considered for this compound at $15 < T < 28$ °K.

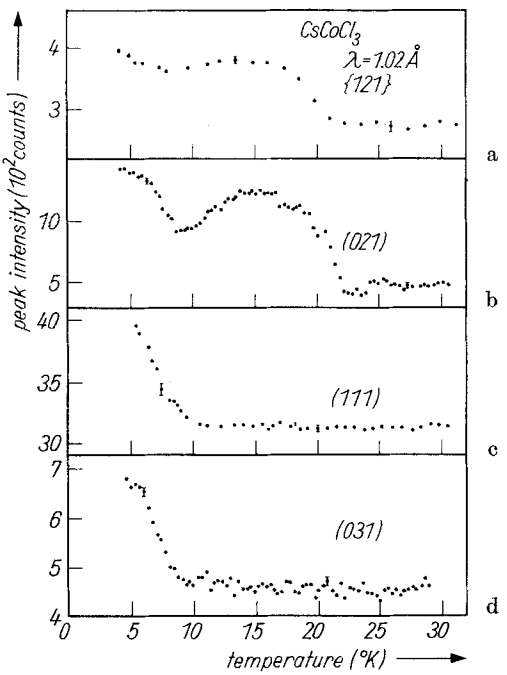

Fig. 3. The peak intensity-temperature curve for the magnetic reflections a) powder {121}, b) single crystal (021), c) single crystal (111), d) single crystal (031)

curves (111) and (031) ($2h + k = -3n$) on the other hand exhibit a transition to magnetic order at 9 °K (Fig. 3). Similar behaviour was found [7] in $CsMnBr_3$ where it was suggested [7] that the upper temperature structure is either of type II or of type III.

Diffraction patterns taken with the sample at RT and at LHeT with 2.4Å neutrons are shown in Fig. 4. Observed integrated intensities of six lines with magnetic contribution were deduced from the LHeT pattern and are listed in Table 4. The magnetic contribution to the {111} line at LHeT was deduced in the following way: $I_{mag} = \alpha I$ (4.2 °K), where $\alpha = [I'(4.2\ °K) - I'(14\ °K)]/I'(4.2\ °K)$ and I' are the integrated intensities observed with a single crystal. The value of α obtained for the {111} line is 0.20 ± 0.01. It can be shown that $n_B = [3.6[\alpha/(1-\alpha)]^{1/2}/f(111)$ where f is the form factor. With the approximation mentioned above for the form factor, $f(111) \approx 0.8$ and $n_B \approx (2.3 \pm 0.3)\,\mu_B$ per Co^{2+} ion.

3. Analysis of the Magnetic Structure

A comparison between the observed integrated intensities of six lines and the intensities calculated for magnetic structures with H-cell which were previously reported (i.e. I, II (or III), V and VI) is given in Table 4. It is quite clear from this table that, of these structures, structure I is the only one consistent with the observed data. In this section, we shall derive the magnetic structure in a systematic way. We shall find that structure I gives the best fit to our data.

The derivation of the most probable magnetic structure is actually a search for a structure of highest symmetry consistent with the neutron diffraction pattern at LHeT.

Assuming that the para- to antiferromagnetic transition is a phase transition of the second order, the space group of the magnetic structure must be a subgroup of the paramagnetic space group. The only maximal subgroup of D^4_{6h}-$P6_3/mmc$ consistent with the H-cell is D^3_{6h}-$P6_3/mcm$ [21]. The enlargement of the cell from the P-hexagonal to the H-hexagonal (the latter cell being consistent with the LHeT pattern) is by a factor of three. The reduction in symmetry is consequently also by a factor of three (the rotational part of D^4_{6h} and D^3_{6h} being of the same order).

Table 3

Magnetic structures in compounds isostructural with $CsNiCl_3$

magnetic structure type	c_0 chains*)	direction of magnetic moment	k-vector relative to P lattice	magnetic space group	magnetic unit cell	reduction in symmetry
I	AF	$\boldsymbol{\mu} \parallel \boldsymbol{c}_0$	1/3 1/3 0	$P6_3'/m'cm'$	(2, 1, 0) (1, 2, 0) (0, 0, 1)	6
II	AF	$\boldsymbol{\mu} \parallel \boldsymbol{c}_0$	1/3 1/3 0	$P6_3'/m'cm'$	(2, 1, 0) (1, 2, 0) (0, 0, 1)	6
III	AF	$\boldsymbol{\mu} \parallel \boldsymbol{c}_0$	1/3 1/3 0	$P6_3'/m'cm$	(2, 1, 0) (1, 2, 0) (0, 0, 1)	6
IV	F	$\boldsymbol{\mu} \parallel \boldsymbol{b}_0$	1/2 0 0	$C_pmc'm'$	(2, 1, 0) (0, 1, 0) (0, 0, 1)	6
V	AF	$\boldsymbol{\mu} \perp \boldsymbol{c}_0$	1/3 1/3 0	$P\bar{6}2'm'$**)	(2, 1, 0) (1, 2, 0) (0, 0, 1)	12
VI	AF	$\boldsymbol{\mu} \perp$ [100]	1/3 1/3 0	$Cm'c2_1'$**)	(2, 1, 0) (0, 3, 0) (0, 0, 1)	36
VII	AF	$\boldsymbol{\mu} \perp \boldsymbol{c}_0$	noncomensurate			

I. With the sequence $+1\ -1\ -1\ +1$ along [110].
II. With the sequence $+1\ -1/2\ -1/2\ +1$ along [110].
III. With the sequence $0\ +1\ -1\ 0$ along [110].
IV. Ferromagnetic b_0, c_0 planes coupled antiferromagnetically.
V. $\boldsymbol{\mu}$ rotates about $\boldsymbol{c}_0$ with a period of $3a_0$ along [110].
VI. $\boldsymbol{\mu}$ rotates about [110] with a period of $3a_0/2$ along $\boldsymbol{b}_0$.
VII. $\boldsymbol{\mu}$ rotates about $\boldsymbol{c}_0$ with a turn angle of about 130° propagating along [110].
*) AF antiferromagnetic, F ferromagnetic.
**) Ferromagnetism is allowed by these groups.

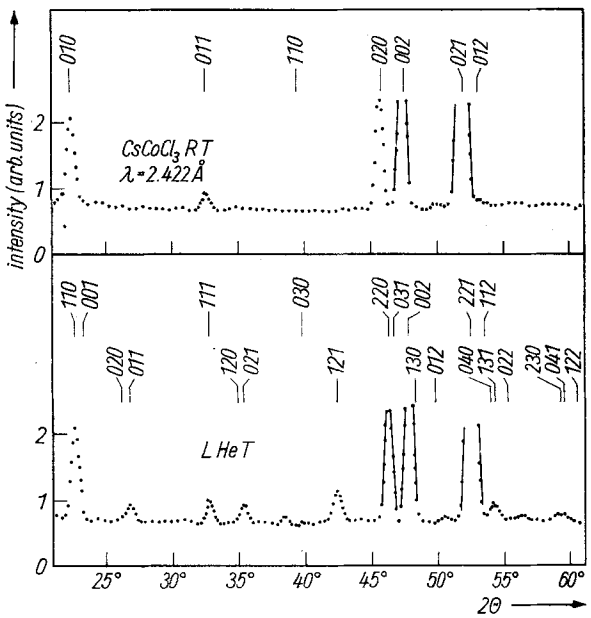

Fig. 4. Neutron ($\lambda = 2.4$ Å) diffraction patterns of $CsCoCl_3$ at room and liquid helium temperature (RT and LHeT). Indexing as in Fig. 1

There are eight magnetic space groups isomorphous with $P6_3/mcm$ [22], namely $P6_3/mcm$, $P6_3/m'cm$, $P6_3'mc'm$, $P6_3'/mcm'$, $P6_3'/m'cm$, $P6_3'/m'cm'$, $P6_3/mc'm'$, and $P6_3/m'c'm'$. Among these only $P6_3/mc'm'$ and $P6_3'/m'cm'$ allow magnetic ordering in the sites 2b and 4d (in which the six Co^{2+} ions are placed in the H-cell, see Table 1b). The structure consistent with $P6_3/mc'm'$ is ferromagnetic with spins parallel to the c-axis. This structure has the P-cell as a unit cell and is therefore inconsistent with the superlattice lines in the LHeT pattern. There are two structures consistent with $P6_3'/m'cm'$. One structure consists of ferromagnetic (spins parallel to c) ab planes stacked antiferromagnetically along c. This structure has the P-cell as a unit cell and is therefore inconsistent with the LHeT pattern. The second structure consistent with $P6_3'/m'cm'$ is shown in Fig. 2. It is identical to structure type I (Table 3) and is consistent with the observed line intensities (Table 4).

Let us now consider structures with the full hexagonal symmetry in which $|\mu_b| \neq |\mu_d|$ (i.e. in which magnetic moments on a 2b position are not equal in magnitude to the magnetic moment on a 4d position). There are only two structures of this sort: $(\mu_b, \mu_d, \mu_d, -\mu_b, -\mu_d - \mu_d)$ and $(0, \mu_d, -\mu_d, 0, -\mu_d, \mu_d)$ where $\mu_\alpha = \boldsymbol{\mu}_\alpha \cdot \hat{\boldsymbol{c}}$ (α = b, d) and the i-th entry gives μ_α in the i-th position (Fig. 3). The latter structure is identical with structure type III and is inconsistent with the observed pattern at LHeT (Table 4). By varying μ_b/μ_d in the former structure it was found that $\mu_b/\mu_d \approx -1$ gave the best agreement with the observed intensities. This value of μ_b/μ_d however corresponds to structure type I.

We can now summarize the results of this section.

(i) Structure type I which has the full hexagonal symmetry fits the observed data.

Table 4

Observed integrated intensities with the sample at LHeT. Calculated intensities for the four H-cell magnetic structures previously reported

$\{hkl\}$	I_{obs}	I_{calc}			
		I	II (III)	V	VI
{011}	18.4 ± 0.9	15.8	16.7	35.2	32.4
{111}	4.1 ± 0.8*)	5.1	0	19.4	0.0
{021}	18.9 ± 0.8	19.8	20.8	15.5	19.8
{121}	29.7 ± 1.2	31.6	33.4	17.7	27.0
{131}	16.0 ± 2.5	19.7	20.7	8.9	15.0
{041}	12.9 ± 1.0	7.9	8.4	3.3	5.9

*) Intensity difference (see text).

(ii) There is no other structure of a higher or an equal symmetry which gives as good a fit to the observed data.

4. Discussion

The RT pattern (Fig. 1) is in agreement with the crystallographic structure found by X-ray analysis [1 to 4]. The x parameter for the position of the Cl^- ions found by least square fitting (Table 1) is 0.155 ± 0.002 in agreement with the value given by Soling [3], which is 0.1545.

The proposed spin structure (Fig. 2) may be considered as a "mixture" (Fig. 5) of two different spin structures. The two structures transform like basis vectors of two different irreducible representations $\Gamma_3(\boldsymbol{k} = [\frac{1}{3}\ \frac{1}{3}\ 0])$ and Γ_3^+ of $P6_3/mmc$. The latter appears in the decomposition of the cube of the former (i.e. $\Gamma_3 \times \Gamma_3 \times \Gamma_3 \supset \Gamma_3^+$). This mixture is therefore [23] allowed according to the theory of second order phase transition (SOPT) of Landau and Lifshitz [24].

The magnetic moment per Co^{2+} ion refined to fit (least squares) our powder data at LHeT is $(3.0 \pm 0.3)\,\mu_B$. The corresponding value deduced from the single crystal data is $(2.3 \pm 0.3)\,\mu_B$ (similar deviation was found [12] in $CsNiCl_3$ where $1.5\,\mu_B$ and $1.05\,\mu_B$ were deduced from powder and single crystal data respectively). These values are somewhat lower than the spin only value which is $3\mu_B$.

We intend to study the "high temperature" structure near T_N, and the nature of the transition from this structure to the LHeT structure.

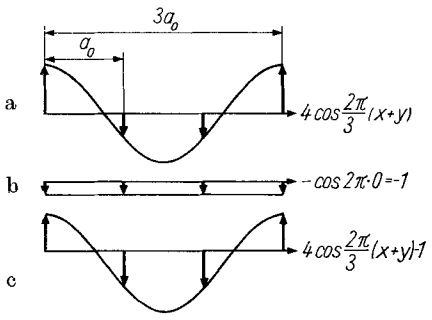

Fig. 5. Spin structures obtained [23] from basis vectors of the representations: a) Γ_3 of $P6_3/mmc$ with $\boldsymbol{k} = (1/3, 1/3, 0)$; b) Γ_3^+ of $P6_3/mmc$ with $\boldsymbol{k} = (0, 0, 0)$; c) the sum of a) and b). The modulating function $\cos(2\pi\boldsymbol{k} \cdot \boldsymbol{r})$ for every structure is given at the right. The spins are shown along the [100] direction in the primitive hexagonal lattice (or along the diagonal of the H-cell, see Fig. 2), a_0 is the lattice translation in the primitive hexagonal lattice

Acknowledgements

We wish to acknowledge Prof. S. Shtrikman of the Weizmann Institute, Dr. S. Goshen and Dr. D. Mukamel of the Nuclear Research Center-Negev for numerous discussions on the application of the theory of SOPT in this work.

References

[1] D. J. W. IJDO, Thesis, Leiden 1960 (unpublished).
[2] H. J. SEIFERT, Z. anorg. allg. Chem. **307**, 137 (1961).
[3] H. SOLING, Acta chem. Scand. **22**, 2793 (1968).
[4] H. F. MCMURDIE, J. DE GROOT, M. MORRIS, and H. E. SWANSON, J. Res. Nat. Bur. Standards A **73**, 621 (1969).
[5] A. N. CHRISTENSEN and G. OLIVER, J. Solid State Chem. **4**, 131 (1972).
[6] V. J. MINKIEWICZ, D. E. COX, and G. SHIRANE, J. Phys. C **32**, 892 (1971).
[7] W. B. YELON, D. E. COX, and V. J. MINKIEWICZ, Bull. Amer. Phys. Soc. **17**, 339 (1972). D. E. COX, private communication.
[8] A. EPSTEIN, J. MAKOVSKY, and H. SHAKED, Solid State Commun. **9**, 249 (1971).
[9] M. STEINER, Solid State Commun. **11**, 73 (1972).
[10] M. EIBSCHUZ, R. C. SHERWOOD, F. S. HSU, and D. E. COX, BNL 17520, to be published.
[11] G. R. DAVIDSON, M. EIBSCHUTZ, D. E. COX, and V. J. MINKIEWICZ, Proc. 17th AIP Ann. Conf. Magnetism and Magnetic Materials, Chicago 1971, Ed. C. D. GRAHAM and S. J. RHYNE, American Institute of Physics, New York 1972 (p. 436).
[12] V. J. MINKIEWICZ, D. E. COX, and G. SHIRANE, Solid State Commun. **8**, 1001 (1970). W. B. YELON and D. E. COX, Phys. Rev. B **6**, 204 (1972). D. E. COX and V. J. MINKIEWICZ, Phys. Rev. B **4**, 2209 (1971).
[13] C. J. GLINKA, V. J. MINKIEWICZ, D. E. COX, and C. P. KHATTAK, to be published.
[14] H. RINNEBERG and H. HARTMAN, J. chem. Phys. **52**, 5814 (1970).
[15] N. ACHIWA, J. Phys. Soc. Japan **27**, 561 (1969).
[16] M. STINER, K. KRUGER, and D. BABEL, Solid State Commun. **9**, 227 (1971).
[17] D. E. COX and V. J. MINKIEWICZ, Acta cryst. A **27**, 494 (1971).
[18] Neutron Diffraction Commission, Acta cryst. A **28**, 357 (1972).
[19] International Tables for X-Ray Crystallography, Kynoch Press, 1952 (p. 18).
[20] R. E. WATSON and A. J. FREEMAN, Acta cryst. **14**, 27 (1971).
[21] J. NEUBÜSER and H. WONDRATSCHEK, Maximal Subgroup of the Space Groups, 2nd printing, April 1968 (unpublished).
[22] W. OPECHOWSKI and R. GUCCIONE, Magnetism IIA, Ed. G. T. RADO and H. SUHL, Academic Press, 1965.
[23] For a more detailed discussion see: M. MELAMUD, H. PINTO, J. MAKOVSKY, and H. SHAKED, An Investigation of the Magnetic Structure of $CsCoCl_3$, NRCN-372 (1974).
[24] L. D. LANDAU and E. M. LIFSHITZ, Statistical Physics, Chap. 14, Addison Wesley Publ. Co., 1958.

(Received March 25, 1974)